

Reoxidation of Bioreduced Uranium Under Reducing Conditions

Jiamin Wan¹, Tetsu K. Tokunaga¹, Joern Larsen¹, Eoin Brodie², Zheming Wang³, Zuoping Zheng¹, Don Herman², Terry C. Hazen¹, Mary K. Firestone², & Stephen R. Sutton⁴

¹Lawrence Berkeley National Laboratory, Berkeley, California, ²University of California, Berkeley, California
³Pacific Northwest National Laboratory, Richland, Washington, ⁴University of Chicago, Chicago, Illinois

Introduction

Strategies under development for bioremediating U-contaminated soil and groundwater rely on injecting organic carbon (OC) into sediments in order to stimulate direct and indirect microbial U(VI) reduction to low solubility U(IV) solids. Although reduction-based remediation will require long-term immobilization, studies to date have yet to demonstrate sustainability of reduced U(IV). When unperturbed by influxes of highly oxidizing TEAs (dissolved oxygen, nitrate and denitrification products that are known to oxidize U(IV)), U(IV) is commonly assumed to be stable in reducing sediments. This study has tested the stability of U bioreduction under sustained reducing conditions for nearly 2 years, and revealed a critical problem in applying OC-based U bioremediation.

Methods

- Soil columns:** (200 mm length, 32 mm ID, 12 replicates) packed with contaminated soil with a U concentration of 206 mg kg⁻¹ obtained from the Natural and Accelerated Bioremediation (NABIR) Program's Field Research Center in Oak Ridge National Laboratory, Tennessee, USA. Na-lactate solution (10.7 mM lactate, 32 mM OC) was infused at pore fluid velocity of 10 mm d⁻¹.
- Measurements in effluents:** concentrations of U, organic carbon and inorganic carbon, CH₄ and CO₂, Fe, Mn, and Ca. pH measurements were obtained in-line at column outlets. Redox potentials were measured within columns with permanently embedded Pt electrodes, and also calculated based on ratios of methane and CO₂ concentrations.
- U oxidation states:** determined non-destructively in soil columns using synchrotron micro-X-ray absorption near edge structure (μ -XANES) spectroscopy.
- Aqueous uranyl species in soil effluents:** determined using fluorescence spectroscopy and lifetime measurements.
- Microbial community analyses:** high density oligonucleotide array analyses, and real-time quantitative PCR analyses.
- Thermodynamic calculations:** Influence of carbonate accumulation on U(IV)/U(VI) redox boundaries.

Results and Discussion

Reductive immobilization of U was completed by day 60:

The effluent U concentrations decreased rapidly (Fig. 1a) as microbial respiration consumed OC (Fig. 1b) and increased (bi)carbonate concentrations (Fig. 1c). 95% of the lactate was consumed, with HCO₃⁻, CO₂, and CH₄ being the dominant products (Table 1). Microbial respiration drove P_{CO2} in soils from 10^{-3.5} up to 10^{-1.5} atm, and average redox potentials down to pe = -3.4 to -4.2 (Table 1). By around day 60, U concentrations declined by 3 orders of magnitude, to less than 30 nM (the U.S. EPA drinking water standard for U is 126 nM). Thus, in-situ reductive immobilization of U appeared successful at this point and in agreement with previous studies.

Bioreduced U was remobilized after day 100, under reducing conditions:

However, upon further permeation with the lactate solution, increased U concentrations in the effluents were observed after about day 100 in all of the columns (Fig. 1a). U concentrations increased 30-fold, back to ≈1 μM by day 200. Steady OC consumption and carbonate and methane production indicated that an active microbial population was sustained (Table 1). The stable low pe (-3.4 to -4.2) and the steady methane production documented that the soils remained very reducing. Thus, U remobilization after day 100 occurred in the presence of sustained microbial populations and reducing conditions.

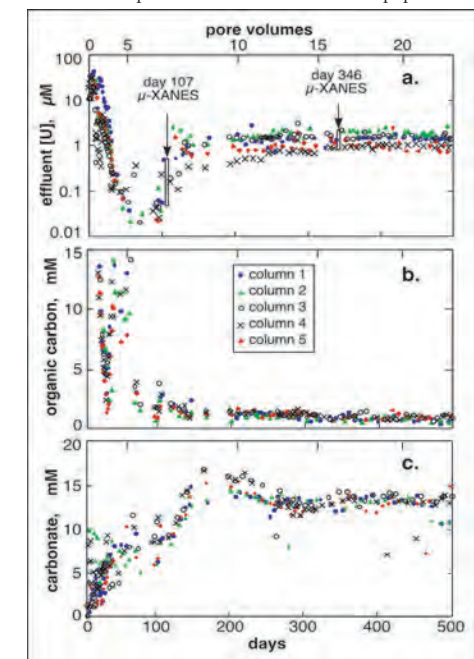


Figure 1. U, OC, and carbonate concentrations (all relative uncertainties < 10%) from 5 representative soil columns. a, U trends show bioreduction completed at ~day 60, reoxidation began at ~day 100, and reached steady-state at ~day 200. Bars indicate times for μ -XANES measurements of U oxidation states. b, OC trends show 95% of injected lactate was being consumed, leaving 1 mM OC in effluents. c, (Bi)carbonate trends show this major product of microbial respiration increased to 15 mM, then decreased to 13 mM after about day 215 because of switching to a lower flow rate (lower rate of OC supply).

| | Influent | Steady-state effluent |
|--|----------|--------------------------|
| pH | 7.2 | 7.4 ± 0.14* |
| redox potential, pe | > 0 | -3.4 ± 1.0*; -4.2 ± 0.3* |
| log ₁₀ (P _{CO2} , atm) | < -3.5 | -1.5* |
| OC (lactate) mM | 32.0 | 1.01 ± 0.25 |
| carbonate mM | 0 | 12.7 ± 1.4 |
| CH ₄ mM | 0 | 10.4 ± 1.9 |
| C mass recovery | | 75% |
| Ca mM | 1.0 | 1.0 ± 0.4 |
| Fe mM | 0 | 0.045 ± 0.005 |
| Mn mM | 0 | 0.035 ± 0.005 |

Table 1. Steady-state solution chemistry (averages and standard deviations from 12 columns). a In-situ pH measurements. b Measured by using Pt electrodes. c Calculated based on measured pH, CO₂ and CH₄ data. d Calculated based on measured bicarbonate and pH data.

U(IV) reoxidation occurred under reducing conditions:

U oxidation states within three soil columns were directly measured using μ -XANES spectroscopy (Fig. 2). Data show 87% (±26%) of the U as U(IV) at day 107, and by day 346 the soil U(IV) declined to 58% (±22%) of the total U. The standard deviations primarily reflect large spatial variability of U(IV) fractions in the soils at the measurement scale (≈ 1 mm³) rather than valence uncertainty of the spectra (≈ 12%). Despite this variability, the two sets of in-situ μ -XANES analyses were significantly different at p = 0.005, demonstrating that previously bioreduced U(IV) was reoxidized.

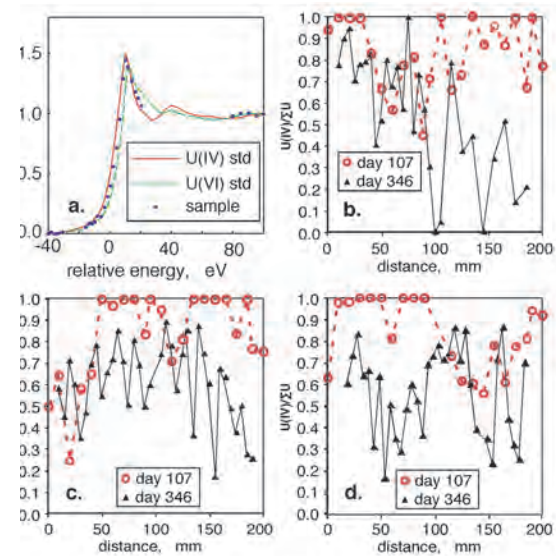
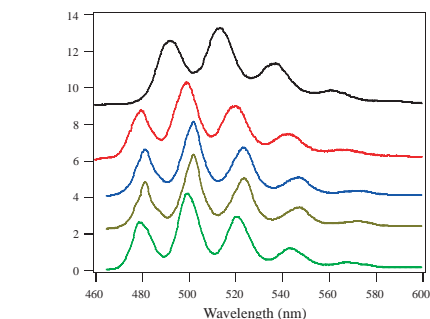


Figure 2. Micro-XANES spectra profiles of U(IV) fractions in 3 soil columns. a, Examples of XANES spectra from U(IV) and U(VI) standards, and from a location within a soil column. b, c, d, profiles from 3 soil columns obtained on days 107 and 346. Note that measurements within soils on the 2 different days were not necessarily obtained at identical locations. (The measurements were performed at GSECARS, Sector 13, Advanced Photon Source, Argonne National Laboratory.)



Uranyl tricarbonate complex is dominant in later effluents:

The uranyl fluorescence spectrum of the effluent sample collected before reduction occurred resembles that of Ca₂UO₂(CO₃)₂ (aq) (nearly 100%), while the spectrum from the reoxidation stage effluent is composed of 61% (UO₂)(CO₃)₃⁴⁻ and 39% Ca₂UO₂(CO₃)₂.

Figure 3. Fluorescence spectra of aqueous uranyl complexes at 6 K, with λ_{ex} = 415 nm. a, uranyl ion [UO₂²⁺]; b, (UO₂)₂(CO₃)₂; c, Ca₂UO₂(CO₃)₂; d, effluent sample collected before reduction; e, effluent sample collected during the steady-state reoxidation stage. Spectra are normalized to the same maximum intensities and offset along the vertical axis. (The measurements were performed at the W.R. Wiley Environmental Molecular Sciences Laboratory.)

A microbial community capable of U reduction remained through the reoxidation phase:

Data from high-density oligonucleotide arrays indicated that functional groups of relevance within the microbial community remained stable as the 16S rDNA amplicon abundance of most *Geobacteraceae* detected did not change significantly (p > 0.05) between the reducing and oxidizing stages. Real-time PCR was used to quantify *Geobacteraceae* 16S rDNA gene copies in soil extracts (Fig. 4), and confirmed array observations that the cell densities of organisms within the *Geobacteraceae* bacteria remained consistent between the reduction and oxidation stages. These results suggest that a microbial community capable of continued U reduction remained through the reoxidation phase and that a loss of microbial functionality was not a factor in U(IV) reoxidation.

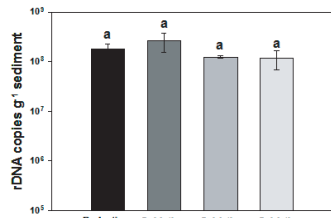


Figure 4. Quantitative PCR determination of *Geobacteraceae* 16S rDNA gene copy numbers in sediment samples taken from columns during net uranium reduction and net uranium oxidation phases. Reduction phase samples represent three random samples taken from homogenized column material (n=3). Oxidation phase samples represent three replicate samples taken from each of three column regions, bottom, middle and top (n=9). Same letters denoted no significant difference (p > 0.05).

Conclusions

The experiments were conducted on historically U contaminated soil supplied with lactate-enriched simulated groundwater, at reasonable groundwater flow-rates, with most measurements obtained non-invasively. The results show that microbial reduced U(IV) is reoxidized under reducing (methanogenic) conditions, while a microbial community capable of reducing U(VI) remained active. Microbial respiration caused increased (bi)carbonate concentrations and formation of stable uranyl carbonate complexes, thereby shifting U(IV)/U(VI) equilibrium to much more reducing potentials. Thus, U remediation by organic carbon based reductive precipitation can be problematic in neutral to alkaline sediments and ground waters.

Reoxidation of U(IV) is thermodynamically favored with increased CO₂ partial pressures: The impact of increased CO₂ partial pressure on U redox transformations is illustrated in Table 2. U(VI)/U(IV) redox potentials shift substantially towards more reducing conditions when CO₂ partial pressure increases from 10^{-3.5} to 10^{-1.0} atm (other conditions constant), and also decrease when calcite is present. Thus, reoxidation of previously reduced U(IV) is thermodynamically favored with increased CO₂ partial pressures within these reducing soils.

| Reactions | Eh ^o (mV) | Eh (mV) at P _{CO2} = | | |
|---|----------------------|-------------------------------|------------------------|------------------------|
| | | 10 ^{-3.5} atm | 10 ^{-1.5} atm | 10 ^{-1.0} atm |
| UO ₂ CO ₃ + H ⁺ + 2e ⁻ → UO ₂ (aq) + HCO ₃ ⁻ | 278 | -14 | -73 | -88 |
| UO ₂ (CO ₃) ₂ ²⁻ + 2H ⁺ + 2e ⁻ → UO ₂ (aq) + 2HCO ₃ ⁻ | 366 | -41 | -159 | -189 |
| UO ₂ (CO ₃) ₃ ⁴⁻ + 3H ⁺ + 2e ⁻ → UO ₂ (aq) + 3HCO ₃ ⁻ | 531 | 8 | -169 | -213 |
| Ca ₂ UO ₂ (CO ₃) ₂ + 3H ⁺ + 2e ⁻ → UO ₂ (aq) + 3HCO ₃ ⁻ + 2Ca ²⁺ | 278 | -156 | -215 | -230 |
| CaUO ₂ (CO ₃) ₂ ²⁻ + 3H ⁺ + 2e ⁻ → UO ₂ (aq) + 3HCO ₃ ⁻ + Ca ²⁺ | 427 | -51 | -169 | -198 |
| Fe(OH) ₃ + 3H ⁺ + e ⁻ → Fe ²⁺ + 3H ₂ O | 976 | -78 | -78 | -78 |
| MnO ₂ (pyrolusite) + 4H ⁺ + 2e ⁻ → Mn ²⁺ + 2H ₂ O | 1220 | 1180 | 1180 | 1180 |

Table 2. Redox reactions and potentials. Eh^o: standard redox potentials. Eh: redox potentials under different P_{CO2} conditions at pH 7.4, Σ(U(VI))_{aq} = 10⁻⁶ M, Fe²⁺ = 4.5 × 10⁻⁶ M, Mn²⁺ = 3.5 × 10⁻⁶ M, and [Ca²⁺] dependent on P_{CO2}.

Acknowledgements

We thank T. DeSantis, D. Joyner, M. Newville, G. Anderson, and S. Baek for technical assistance. Funding was provided by the U. S. Department of Energy (DOE), NABIR Program, the Basic Energy Sciences (BES) Geosciences Program, GeoSoilEnviroCARS (GSECARS), Advanced Photon Source (APS), Argonne National Laboratory. GSECARS is supported by the National Science Foundation - Earth Sciences, DOE- Geosciences and the State of Illinois. Use of the APS was supported by the DOE BES, Office of Energy Research. Fluorescence spectroscopic measurements were performed at the W.R. Wiley Environmental Molecular Sciences Laboratory, a national scientific user facility sponsored by the DOE's Office of Biological and Environmental Research.